1 <div align="center">Supplementary Information for</div>

2 <div align="center">**Determining Monolignol Oxifunctionalization by Direct Infusion**</div>

3 <div align="center">**Electrospray Ionization Tandem Mass Spectrometry**</div>

4

5 Rannei Skaali,[*a] Hanne Devle,[a] Katharina Ebner,[b] Dag Ekeberg,[a] and Morten Sørlie[a]

6 [a]Faculty of Chemistry, Biotechnology and Food Science, Norwegian University of Life Sciences, Christian Magnus

7 Falsens vei 18, 1433, Ås, Norway.

8 [b]Bisy GmbH, Wünschendorf 292, 8200 Hofstätten an der Raab, Austria

9 * Correspondence to: rannei.skaali@nmbu.no

10 **This Supplementary Includes:**

11 **1. List of Supplementary Figures and Tables**

12 **Fig. S1:** Isotope labeling experiment.

13 **Fig. S2:** Ion suppression.

14 **Fig. S3:** MS/MS analysis of 4-propylguaiacol and 4-propylsyringol with respective oxifunctionalized products.

15 **Fig. S4:** MS/MS analysis of UPO-based oxifunctionalized monolignols.

16 **Fig. S5:** Full scan DI-ESI-MS of *Cma*UPO-I catalyzed biotransformation of 4PS at 37°C.

17 **Table S1:** Activity of commercial UPO library on the substrates 5-nitro-1,3-benzodioxol (NBD) and 4-nitroanisol (4-

18 NA).

19 **Table S2:** Monolignol calibration curves.

20

2. Preliminary Enzyme Selection

Preliminary enzyme selection was performed using 41 different proteins of the class UPO produced by bisy GmbH (Wuenschendorf, Hofstaetten a. d. Raab, AUT). Briefly, the activity of the enzymes on two different substrates, 5-nitro-1,3-benzodioxol (NBD) and 4-nitroanisol (4-NA), was determined in a microplate-based high-throughput (HT) approach using spectrophotometric assays. Both substrates represent small aromatic molecules reminiscent of guaiacol units of lignin-containing methyl groups liable for elimination via demethylation, which is a desirable reaction for the degradation as well as functionalization of lignin.[1] O-dealkylation of NBD to 4-nitrocatechol is a well-established reaction for determining the peroxygenase activity of UPOs and the corresponding HT assay is routinely used for enzyme engineering approaches.[2-4] However, the methylene group in NBD is bound in an acetal moiety, which makes it highly activated (electron-rich) and therefore favored for demethylation. In contrast, the conversion of 4-NA to 4-nitrophenol represents the elimination of a non-activated methyl group via demethylation. The activity of *Aae*UPO on this substrate has previously been shown with analysis of product formation using HPLC.[5] Alternatively, we used an HT microplate-based approach for detecting the production of 4-Nitrophenol at 400 nm in a spectrophotometer.
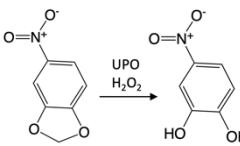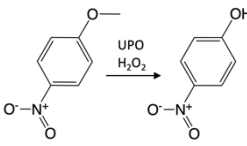
For both substrates enzymatic activity was determined in kinetic measurements following product formation at 425 nm and 400 nm for NBD and 4-NA, respectively. For NBD and 4-NA assay specific enzyme activity was calculated using the volumetric activity (U/mL) determined with the extinction coefficient of the reaction product as described in literature (NBD: $\varepsilon(425) = 9700 \ 1/M*cm^2$) or the change in absorbance over time ($\Delta Abs_{425}/min$), respectively, normalized to protein amount determined by standard Bradford assay (Table S1). For the conversion of NBD to 4-nitrocatechol, the reaction conditions were as follows: 100 mM potassium phosphate buffer pH 7.0, 123 μM NBD, 1 vol% ACN, and 1 mM H_2O_2 at room temperature (RT). For the conversion of 4-NA to 4-nitrophenol, the reaction conditions were as follows: 100 mM Trizin buffer pH 7.5, 0.7 mM 4-NA, 5 vol% ACN, and 0.35 mM H_2O_2 at RT. Reactions were done in a total volume of 200 μL in 96-well microtiter plates (polystyrol, transparent, F-bottom) using 20 μL or 60 μL protein suspensions (in an appropriate dilution) for NBD and 4-NA, respectively. Plates were stirred briefly, and the initial absorptions were recorded using a plate reader (SpectraMax ABS Plus, Molecular Devices, Sunnyvale, CA, USA) for 5 minutes and the initial linear range of the curve plotting the absorbance against time was used for the calculation of enzymatic activity.

Based on the activity on both substrates one enzyme of each family was selected for further work (Table 1, bold), whereby the activity of the enzyme *Aae*UPO (model UPO from *Agrocybe aegerita*) (Table S1, grey) was evaluated as control. For the "long" class family *Cma*UPO-I was chosen, which shows the highest activity on both substrates for all tested "long" UPOs. For the "short" class family an enzyme showing only average activity on the substrates was selected, *Hsp*UPO. However, for this UPO a crystal structure as well as a rather broad spectrum of substrates was recently published.[6, 7]

3. Supplementary Tables

Table S1: Activity of 41 different UPOs on the substrates 5-nitro-1,3-benzodioxol (NBD) and 4-nitroanisol (4-NA). Systematic name of the enzymes, the corresponding NCBI accession number, as well as the family classification of "long" or "short" UPO are given. UPOs used for further work are highlighted in bold. Activities of the model UPO from *Agrocybe aegerita* (*Aae*UPO) were evaluated as a control and are given in grey.

UPO Systematic Name	NCBI accession number	Family	NBD conversion [$U*mg_{Protein}^{-1}$]	4-NA conversion [$\Delta Abs_{425}*mL*min^{-1}*mg^{-1}$]
*Gma*UPO-II[14]	KDR72024.1	L	60.08	63.20
*Lam*UPO[7]	KIK06072.1	L	50.48	31.56
*Hcy*UPO[7]	KIM43689.1	L	n.d.	6.29
*Abr*UPO-II[15]	OJJ73116.1	S	1849.28	5270.06
HspUPO[12,16]	**7O1R_A**	**S**	**77.44**	**1849.80**
*Pan*UPO[7]	XP_001911526.1	S	130.28	0.67
*Dsp*UPO-I[7]	OTB17553.1	S	4288.02	2403.11
*Atu*UPO[7]	XP_035359174.1	S	93.51	2451.53
*Ani*UPO-II[7]	XP_001390900.2	S	495.02	2036.39
*Alu*UPO[7]	XP_041545399.1	S	1789.86	790.70
*Hsp*UPO-II[7]	OTB02684.1	S	n.d.	90.26
*Rne*UPO[7]	GAP92448.1	S	453.12	55.44
*Dsp*UPO-II[7]	OTB09996.1	S	1416.77	2438.99
*Aac*UPO[7]	XP_020060613.1	S	257.02	477.05
*Gma*UPO-I[16,17]	KDR77412.1	L	21.63	19.71
*Cab*UPO-III[16]	RXW15716.1	L	1018.97	347.20
CmaUPO-I[16]	**TFK24496.1**	**L**	**1105.40**	**603.65**
*Cma*UPO-II[16]	TFK18510.1	L	170.47	0.68
*Lsp*UPO-II[16]	KXN91485.1	L	2266.69	13.48
*Gdi*UPO-II[15]	PPR06026.1	L	n.d.	0.17
*Gdi*UPO[16]	PPQ67339.1	L	25.50	1.83
*Cmi*UPO[16]	TEB20562.1	L	45.73	1.23
*Ano*UPO[16]	KAB8223135.1	S	88.37	1.16
*Glu*UPO[16]	KIK53163.1	S	90.40	96.40
*Dbi*UPO[16]	THV03356.1	S	232.54	2268.10
*Abr*UPO-I[16]	OJJ67899.1	S	389.74	3372.91
*Aps*UPO[16]	XP_031917627.1	S	24.46	0.84
*Abo*UPO[16]	XP_022384340.1	S	21.80	0.75
*Sch*UPO[16]	KFA56383.1	S	n.d.	20.43
*Cab*UPO-IV[15]	RXW17550.1	L	640.13	n.d.
*Mfu*UPO[7]	KAF9443253.1	L	1005.68	n.d.
*Sst*UPO-II[7]	KIJ30606.1	L	48.40	n.d.
*Ela*UPO[7]	EMR65404.1	S	n.d.	9.17
*Msp*UPO[7]	RYP65438.1	S	n.d.	45.54
*Psp*UPO[7]	KFY04896.1	S	n.d.	n.d.
*Sni*UPO[7]	KZS95554.1	L	41.55	0.78
*Ssu*UPO[7]	KZT37902.1	S	110.75	n.d.
*Cab*UPO-V[7]	RXW17616.1	L	43.37	n.d.
*Cab*UPO-VII[7]	RXW15623.1	L	19.68	n.d.
*Mve*UPO[7]	KAF7328405.1	L	57.85	n.d.
*Mor*UPO[7]	KAG7088824.1	S	220.36	1610.94
*Aae*UPO[1]	B9W4V6.1	L	10791.95	3950.41

58

Table S2: Monolignol calibration curves. We employed linear regression (y = ax + b) to construct monolignol calibration curves, assuming a linear relationship between monolignol concentration (explanatory variable) and intensity (response variable). The R^2 (%) is provided for each calibration curve.

Monolignol	α	β	R^2 (%)
4-propylphenol	4.99×10^4	4.19×10^5	99.59
4-hydroxybenzoic acid	4.39×10^4	2.61×10^5	99.57
4-(3-hydroxypropyl)phenol[a]	7.74×10^3	1.20×10^5	97.15
4-proyplbenzene-1,2-diol[a]	1.81×10^2	-1.58×10^3	99.69
4-propylbenzene-1,3-diol[a]	1.74×10^2	1.05×10^3	99.66
4-(1-hydroxypropyl)phenol[a]	7.73×10^0	-6.44×10^1	96.06
4-(2-hydroxypropyl)phenol[a]	6.21×10^1	1.29×10^3	99.05
3-(4-hydroxyphenyl)propanal[b]	7.63×10^2	3.23×10^4	91.01
3-(4-hydroxyphenyl) propan-1-one[c]	-	-	-
3-(4-hydroxyphenyl) propan-2-one	8.99×10^1	2.61×10^3	99.33
3-(4-hydroxyphenyl)propanoic acid	6.65×10^4	-1.44×10^5	99.04
4-propylguaiacol	9.42×10^3	3.51×10^5	76.70
4-hydroxy-3-methylbenzoic acid	6.75×10^4	7.44×10^4	98.26
4-(3-hydroxypropyl)-2-methoxyphenol[a]	6.08×10^3	1.11×10^5	97.26
3-(4-hydroxy-3-methoxyphenyl)propanal[b]	5.45×10^2	7.53×10^3	85.05
1-(4-hydroxy-3-methoxyphenyl)propan-1-one	2.66×10^2	1.13×10^4	97.33
1-(4-hydroxy-3-methoxyphenyl)propan-2-one	1.46×10^1	1.58×10^3	98.68
3-(4-hydroxy-3-methoxyphenyl)propanoic acid	6.75×10^4	-2.70×10^4	97.68
4-propylsyringol	5.78×10^3	3.51×10^4	99.73
4-hydroxy-3,5-dimethoxybenzoic acid	3.00×10^4	1.61×10^5	99.90
4-(3-hydroxypropyl)-2,6-dimethoxyphenol[a]	8.93×10^2	7.24×10^4	96.44
3-(4-hydroxy-3,5-dimethoxyphenyl)propanal[b]	2.02×10^3	1.83×10^4	99.03
1-(4-hydroxy-3,5-methoxyphenyl)propan-1-one	2.06×10^2	1.69×10^3	99.92
1-(4-hydroxy-3,5-methoxyphenyl)propan-2-one	1.69×10^1	1.06×10^3	99.15
3-(4-hydroxy-3,5-dimethoxyphenyl)propanoic acid	1.10×10^5	1.41×10^5	99.99

[a] Monolignols comprising a hydroxyl functional group were quantified at a lower flow rate (0.1 mL/min) compared to the other monolignols (0.3 mL/min) to ensure accurate concentration estimates.

[b] We utilized the water adduct of the aldehyde monolignols to achieve accurate quantification. Additionally, this approach facilitated the quantification of potential mixtures of ketones and aldehydes resulting from monolignol biotransformation.

[c] Establishing a calibration curve for 3-(4-hydroxyphenol)propan-1-one proved challenging, as we were unable to obtain reliable signals.
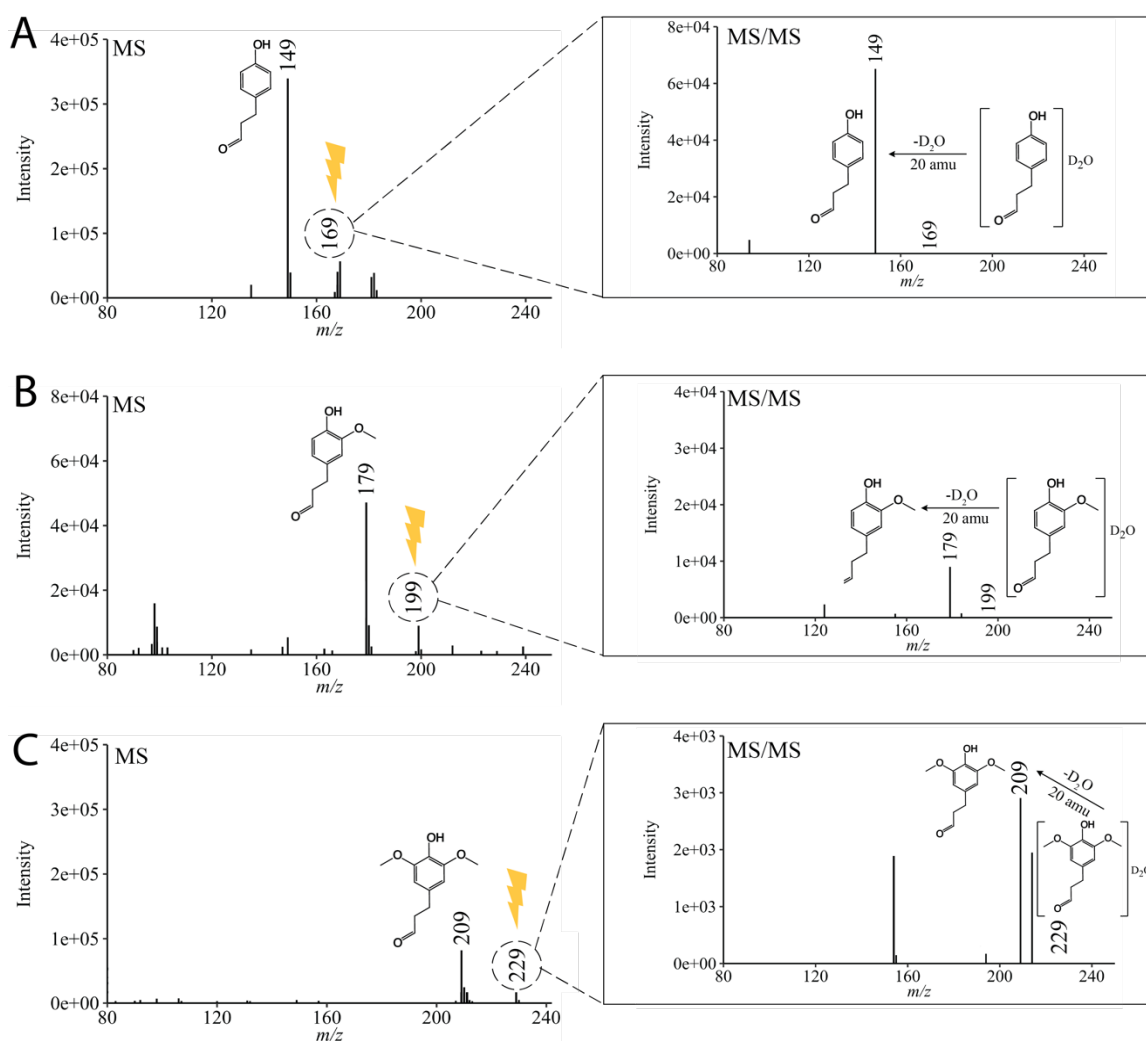
4. Supplementary Figures

Fig. S1: Isotope labeling experiments. 50 µg/mL monolignol aldehyde was dissolved in 50% ACN and 50% D_2O with 150 mM NH_4OH, assuming the formation of the heavy water adduct. Colliding the ions of the molecular species with He gas generated a mass loss of 20 amu, most likely corresponding to the loss of D_2O. Ions generating a signal 2% or less relative to the base peak are omitted for clarity. **(A)** 3-(4-hydroxyphenyl)propanal. NL: 3.69 × 10^5 (MS) and 5.23 × 10^4 (MS/MS). **(B)** 3-(4-hydroxy-3-methoxyphenyl)propanal. NL: 5.00 × 10^4 (MS) and 5.05 × 10^3 (MS/MS). **(C)** 3-(4-hydroxy-3,5-dimethoxyphenyl)propanal. NL: 6.72 × 10^4 (MS) and 1.96 × 10^3 (MS/MS).
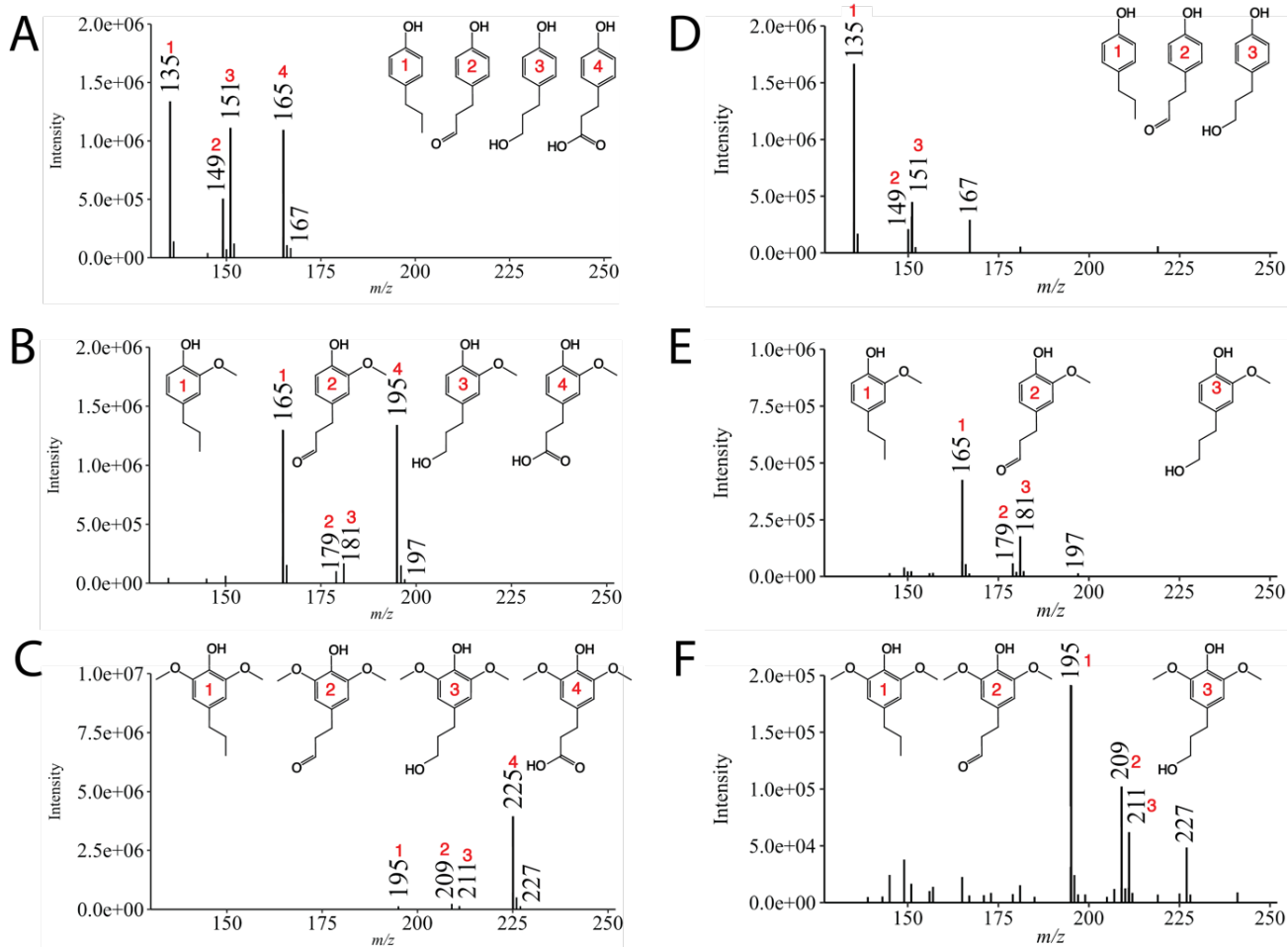
Fig. S2: Ion suppression. Standard solution mixtures comprising the monolignols and the corresponding C$_\gamma$ oxidized products. The exclusion of carboxylic acid compounds from the mixtures resulted in changes to the ion intensities of other compounds, indicating ion suppression likely caused by carboxylic acid monolignols. Ions contributing a signal representing 2% or less relative to the base peak are omitted to enhance clarity. **(A)** 4PP and its C$_\gamma$ oxidized monolignols. NL: 1.33 × 10^6. **(B)** 4PG and its C$_\gamma$ oxidized monolignols. NL: 1.34 × 10^6. **(C)** 4PS and its C$_\gamma$ oxidized monolingols. NL: 3.92 × 10^6. **(D)** 4PP and its C$_\gamma$ oxidized monolignols excluding 3-(4-hydroxyphenyl)propanoic acid. NL: 2.15 × 10^6. **(E)** 4PG and its C$_\gamma$ oxidized monolignols excluding 3-(4-hydroxy-3-methyoxyphenyl)propanoic acid. NL: 4.24 × 10^5. **(F)** 4PS and its C$_\gamma$ oxidized monolignols excluding 3-(4-hydroxy-3,5-dimethyoxyphenyl)propanoic acid. NL: 1.91 × 10^5.
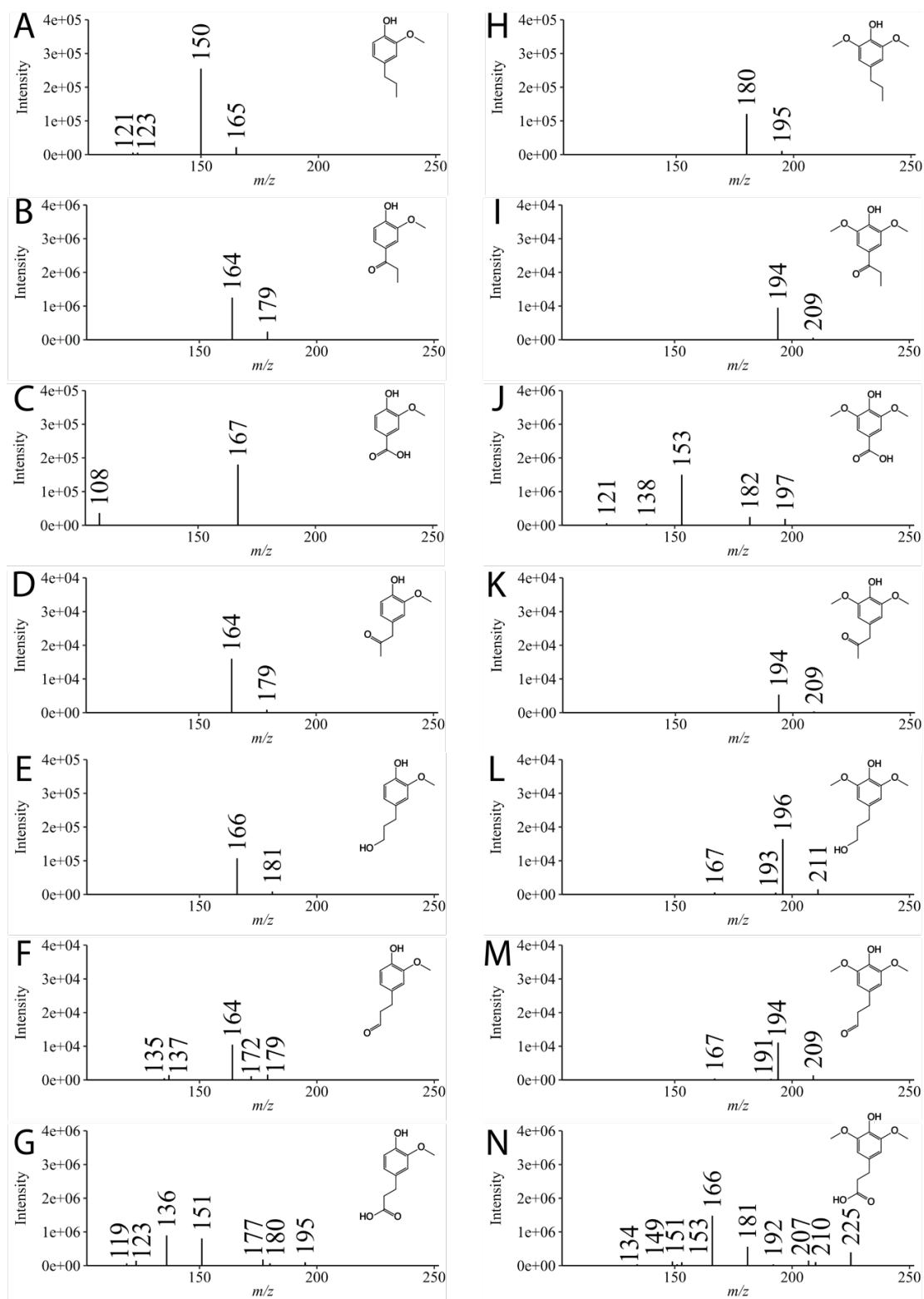
68

Fig. S3: MS/MS analysis of 4-propylguaiacol and 4-propylsyringol with respective oxifunctionalized products. For clarity, ions producing a signal at 2% or lower relative to the base peak are intentionally excluded. **(A)** 4-propylguaiacol (NL = 2.53 × 10^5). **(B)** 1-(4-hydroxy-3-methoxyphenyl)propane-1-one (NL = 1.23 × 10^6). **(C)** 4-hydroxy-3-dimethoxybenzoic acid (NL = 1.70 × 10^6). **(D)** 1-(4-hydroxy-3-methoxyphenyl)propane-2-one (NL = 1.58 × 10^4). **(E)** 4-(3-hydroxypropyl)-2-methoxyphenol (NL = 1.05 × 10^5). **(F)** 3-(4-hydroxy-3-methoxyphenyl)propanal (NL = 1.03 × 10^4). **(G)** 3-(4-hydroxy-3-methoxyphenyl)propanoic acid (NL = 8.77 × 10^5). **(H)** 4-propylsyringol (NL = 1.19 × 10^5). **(I)** 1-(4-hydroxy-3,5-methoxyphenyl)propane-1-one (NL = 9.32 × 10^3). **(J)** 4-hydroxy-3,5-dimethoxybenzoic acid (NL = 1.48 × 10^6). **(K)** 1-(4-hydroxy-3,5-methoxyphenyl)propane-2-one (NL = 5.17 × 10^3). **(L)** 4-(3-hydroxypropyl)-2,6-dimethoxyphenol (NL = 1.62 × 10^4). **(M)** 3-(4-hydroxy-3,5-dimethoxyphenyl)propanal (NL = 1.10 × 10^4). **(N)** 3-(4-hydroxy-3,5-dimethoxyphenyl propanoic acid (NL = 1.46 × 10^6).
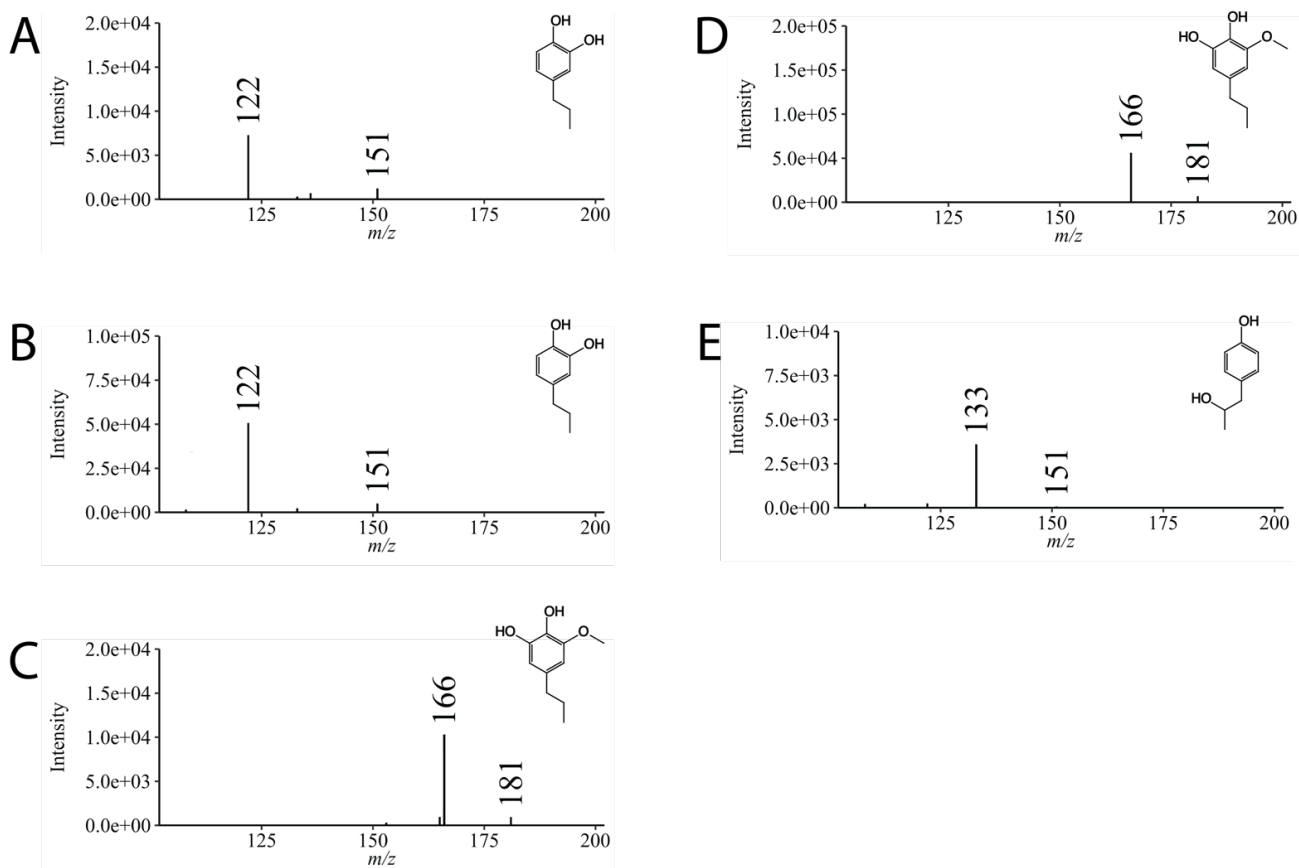
69

7

Fig. S4: MS/MS analysis of UPO-based oxifunctionalized monolignols. To ensure clarity, ions with a signal constituting 2% or less relative to the base peak are intentionally excluded. **(A)** 4-propylbenzene-1,2-diol produced from 4PP catalyzed by *Hsp*UPO (NL = 5.02×10^4). **(B)** *Hsp*UPO catalyzed the oxifunctionalization of 4PG producing 4-propylbenzene-1,2-diol (NL = 7.19×10^3). **(C)** Proposed production of 3-methoxy-5-propylbenzene-1,2-diol in the *Hsp*UPO catalyzed oxifunctionalization of 4PG (NL = 5.52×10^4). This assumption is grounded in logical reasoning; we lack standards to validate or confirm it. **(D)** *Hsp*UPO catalyzed the demethylation of 4PS, proposedly producing 3-methoxy-5-propylbenzene-1,2-diol (NL = 1.02×10^4). We do not have standards to validate or confirm this assumption, which is grounded in logical reasoning. **(E)** 4-(2-hydroxypropyl)phenol was produced as a result of *Cma*UPO-I catalyzed biotransformation of 4PP (NL = 3.56×10^3).
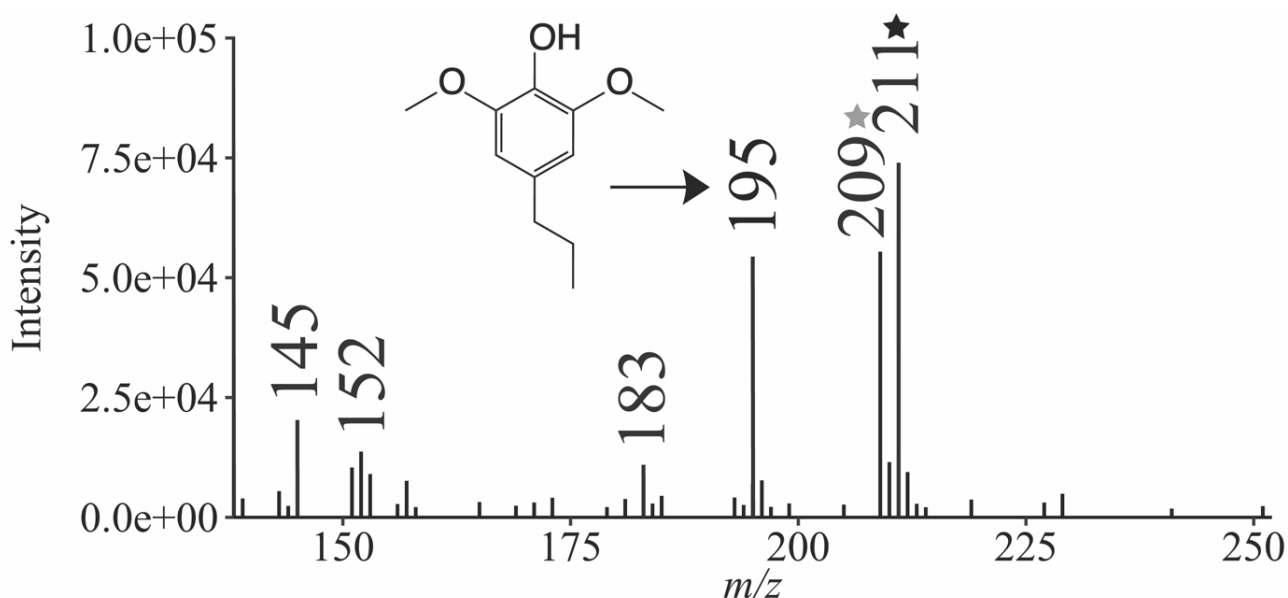

Fig. S5: Full scan DI-ESI-MS of *Cma*UPO-I catalyzed biotransformation of 4PS at 37℃. Pseudo-molecular ions were detected in the *m/z* 70-2000 range. Only [M-H]⁻ ions that generated a signal above 2% relative to the base peak are presented for clarity. *Cma*UPO-I facilitated the hydroxylation of 4PS (m/z 195) at 37℃, resulting in a potential isomeric mixture of 4PS with a hydroxyl group (annotated by a black star, *m/z* 211). Moreover, hydroxylated compounds were further biotransformed into the respective ketones and aldehyde (annotated by a grey star, *m/z* 209). Quantification was challenging due to the isomeric mixtures, however, the intensities of *m/z* 211 and *m/z* 209 were notably increased compared to the controls. NL: 1.30×10^5.

70

8

5. Supplementary References

1.   L. Zou, B. M. Ross, L. J. Hutchison, L. P. Christopher, R. F. Dekker and L. Malek, *Enzyme Microb Technol*, 2015, **73-74**, 44-50.
2.   M. Poraj-Kobielska, M. Kinne, R. Ullrich, K. Scheibner and M. Hofrichter, *Analytical Biochemistry*, 2012, **421**, 327-329.
3.   P. Molina-Espeja, E. Garcia-Ruiz, D. Gonzalez-Perez, R. Ullrich, M. Hofrichter and M. Alcalde, *Appl Environ Microbiol*, 2014, **80**, 3496-3507.
4.   M. Dolz, D. T. Monterrey, A. Beltrán-Nogal, A. Menés-Rubio, M. Keser, D. González-Pérez, P. G. de Santos, J. Viña-González and M. Alcalde, in *Methods in Enzymology*, ed. H. Renata, Academic Press, 2023, vol. 693, pp. 73-109.
5.   M. Kinne, M. Poraj-Kobielska, S. A. Ralph, R. Ullrich, M. Hofrichter and K. E. Hammel, *J Biol Chem*, 2009, **284**, 29343-29349.
6.   L. Rotilio, A. Swoboda, K. Ebner, C. Rinnofner, A. Glieder, W. Kroutil and A. Mattevi, *Acs Catal*, 2021, **11**, 11511-11525.
7.   A. Swoboda, L. J. Pfeifenberger, Z. Duhović, M. Bürgler, I. Oroz-Guinea, K. Bangert, F. Weißensteiner, L. Parigger, K. Ebner, A. Glieder and W. Kroutil, *Angewandte Chemie International Edition*, 2023, **62**, e202312721.